Appl. Phys. B
DOI 10.1007/s00340-013-5379-4

Applied Physics B
Lasers and Optics

Sub-ppb detection of formaldehyde with cantilever enhanced photoacoustic spectroscopy using quantum cascade laser source

C. B. Hirschmann · J. Lehtinen · J. Uotila · S. Ojala · R. L. Keiski

Received: 5 December 2012 / Accepted: 15 February 2013

Abstract A novel cantilever enhanced photoacoustic spectrometer with mid-infrared quantum cascade laser was applied for selective and sensitive formaldehyde (CH_2O) gas measurement. The spectrum of formaldehyde was measured from 1,772 to 1,777 cm^{-1} by tuning the laser with a spectral resolution of 0.018 cm^{-1}. The band at 1,773.959 cm^{-1} was selected for data analysis, at which position the laser emitted 47 mW. In univariate measurement, the detection limit (3σ, 0.951 s) and the normalized noise equivalent absorption coefficient (3σ) for amplitude modulation (AM) were 1.6 ppbv and 7.32×10^{-10} W cm^{-1} $(Hz)^{-1/2}$ and for wavelength modulation (WM) 1.3 ppbv and 6.04×10^{-10} W cm^{-1} $(Hz)^{-1/2}$. In multivariate measurement, the detection limit (3σ) can be as low as 901 pptv (1,773.833–1,774.085 cm^{-1}, 15 spectral points each 0.951 s) for AM and 623 pptv (1,773.743–1,774.265 cm^{-1}, 30 spectral points each 0.951 s) for WM. Because measurement time increases in multivariate measurement, its application is justified only when interferents need to be resolved. Potential improvements of the system are discussed.

C. B. Hirschmann (✉) · S. Ojala · R. L. Keiski
Mass and Heat Transfer Process Laboratory,
Department of Process and Environmental Engineering,
University of Oulu, 90014 Oulu, Finland
e-mail: christian.hirschmann@oulu.fi

C. B. Hirschmann · S. Ojala
Photonics and Measurement Solutions, VTT Technical Research Centre of Finland, Kaitoväylä 1, 90571 Oulu, Finland
e-mail: christian.hirschmann@vtt.fi

J. Lehtinen
Laboratory of Optics and Spectroscopy, Department of Physics and Astronomy, University of Turku, Vesilinnantie 5, 20014 Turku, Finland

J. Uotila
Gasera Ltd., Tykistökatu 4, 20520 Turku, Finland

1 Introduction

Formaldehyde is a frequently used chemical in industry and essential for the production of resins and plastics. Resins are used in adhesives, in finishing products and for instance in MDF fiberboard production. These are commodities typically used in household furniture and paints. In addition to environmental formaldehyde emissions during production, it can be released to the indoor air from the products as well. Especially in indoors and urban areas, formaldehyde can affect human health and cause discomfort, irritation of the eyes, nose, and throat, sneezing, coughing and at elevated concentrations finally death [1–4]. Formaldehyde is toxic whether it is inhaled, eaten or exposure occurred via skin contact [5], it is mutagen, possibly carcinogen [1, 4] and it contributes to the "sick building syndrome" [4]. In addition, formaldehyde itself is suspected to be a biomarker of lung and breast cancer [6, 7]. In Finland, the occupational health limit for 8 h exposure is 0.37 mg m^{-3} ($\sim$300 ppbv) [8], but already at this concentration workers may suffer from slight eye, skin or throat irritation [3]. In urban areas levels of formaldehyde of 3–25 ppb are typical, in normal indoor conditions 10–80 ppb and in polluted indoor conditions 80–300 ppb [4]. By now, a general replacement for formaldehyde has not been found and its utilization continues. Therefore, it is important to develop reliable and accurate measurement technology with online capability. Potential formaldehyde measurement applications are versatile and include industrial and process gas measurement, environmental monitoring, and indoor and urban air quality monitoring as well

Published online: 13 March 2013

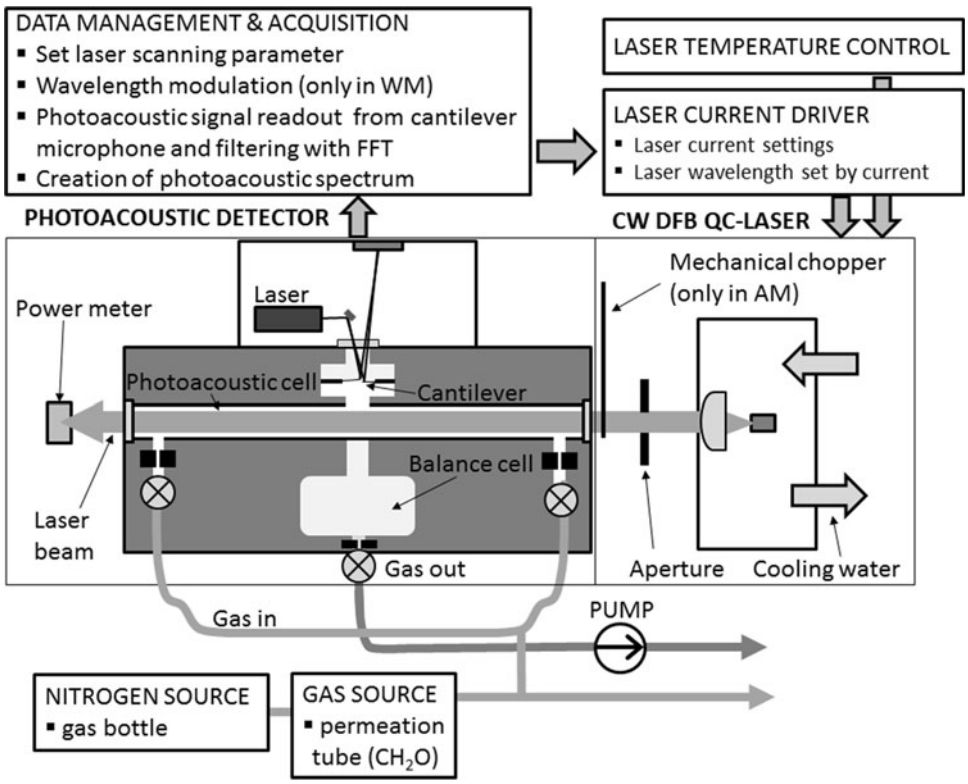

Fig. 1 Schematic of the measurement setup

as biomedical applications, such as breath gas analysis or cancer detection.

Few years ago, a novel microphone based on a silicon cantilever was developed. The theory and the signal model are reported in [9–11]. Various setups were built based on the cantilever microphone and are described in [12, 13] with broad band light source, in [14] with light emitting diode, in [15–19] with diode lasers, and in [20–22] with FT-IRs. Alternative cell designs as the differential setup are reported in [23–27]. A sensitive comparison to other microphones is given in [28]. The advantages of the cantilever microphone are its wide dynamic range and the improved sensitivity as compared to traditional condenser microphones [10, 27].

In this article, a novel cantilever enhanced photoacoustic setup with mid-infrared quantum cascade laser (QCL) is reported. The performance of the system is demonstrated by the trace gas detection of formaldehyde.

2 Experimental

2.1 Measurement setup and parameters

The setup combined a cantilever enhanced photoacoustic cell (Gasera PA201) and a continuous wave (CW) distributed feedback (DFB) quantum cascade laser (QCL) (III-V lab, tunable over 1,772–1,777 cm^{-1}). The QCL chip was fixed in a commercial QCL mount (ILX Lightwave LDM 4872) and the temperature adjusted to 18 °C with thermoelectric temperature controller (Newport Model 350) and water cooling. The emitted light beam was collimated by an aspheric lens and guided through the photoacoustic cell, which had a cylindrical shape with 4 mm diameter and 95 mm length. In case of amplitude modulation (AM), a mechanical chopper was placed in between the lens and the cell. At the end of the cell, the transmitted power was registered with a laser power meter (Thorlabs S302C). The laser was supplied by the current driver (ILX Lightwave LDX-3232). Sample gas was drawn in the cell with a gas exchange unit including pump. The data management and acquisition system was reading the digital, time domain read-out signal from the displacement of the cantilever, FFT transformed it to the frequency domain using power spectrum and recorded the peak height at the modulation frequency simultaneously with the laser current. The photoacoustic spectrum can be reconstructed from the photoacoustic signal and the laser drive current, because the current is proportional to the laser wavelength. Figure 1 shows the schematic of the measurement setup.

Measurements were carried out in amplitude as well as in wavelength modulation (WM). For AM, the mechanical chopper (tuning fork) operating at 135 Hz was used. In WM, the modulation frequency was set to be 70 Hz with a triangular waveform and the signal was picked up at the second harmonic ($2f_{mod}$) at 140 Hz. The sample gas

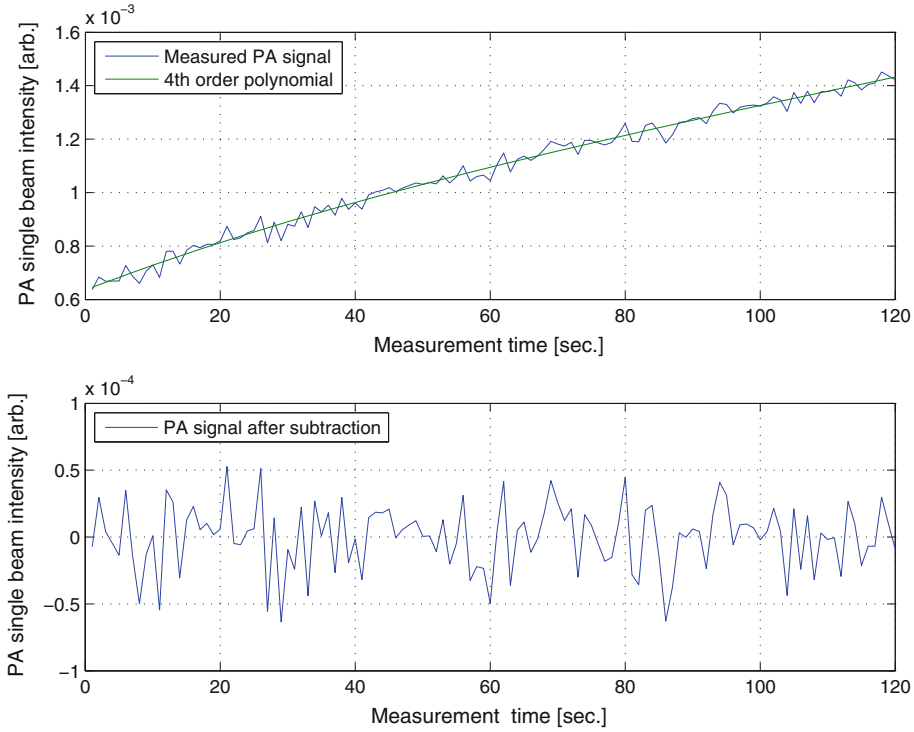

Fig. 2 *Upper graph* one example of the photoacoustic signal records of nitrogen (recorded at 450 mA laser current and 2.8 mW laser power) and its fourth-order polynomial fit. The signal increase over time is due to desorption of water from the cell interior. *Lower graph* nitrogen signal after subtraction of the fit

pressure in the cell was 350 mbar and the cell temperature 50 °C.

2.2 Gas supply

Formaldehyde was measured in a concentration of two parts in 10^6 by volume (ppmv). The 2 ppmv formaldehyde in nitrogen analyte gas mixture was generated with the help of a permeation tube system (Kin-Tek FlexStream™ Gas Standards Generator). Formaldehyde is known to stick quickly on surfaces, therefore all the tubing was kept as short as possible. Each time before filling the photoacoustic cell, the whole set-up was purged with analyte gas for approximately 10 min to avoid contamination, e.g. water vapor to be present in the cell and to stabilize the formaldehyde concentration.

3 Results and discussion

3.1 Data processing and noise characterization

Noise characterization of the system was done with the laser working in AM to include all possible noise sources. The photoacoustic cell was filled with nitrogen up to a pressure of 350 mbar and the photoacoustic signal was measured with different laser powers varying from 1.6 to 43.3 mW by altering the laser input current. For each laser power, the photoacoustic signal was recorded over about 2 min with a single measurement time of 0.951 s. Figure 2 shows one of the photoacoustic signal records of nitrogen (recorded at 450 mA laser current and 2.8 mW laser power). The photoacoustic signal increased during the 2 min recording time, as it can be seen in Fig. 2. Water molecules desorbing from the cell interior to the gas phase are causing the increase in signal. To be able to characterize the noise of the photoacoustic measurement system, the water caused signal increase needs to be removed. This is done by a fourth-order polynomial fit that is subtracted from the measurement data. The residual of the subtraction is the variation in nitrogen signal that is as well shown in Fig. 2. The standard deviation was calculated from ten successive nitrogen signal values, to avoid possible water signal residuals biasing the standard deviation value. Finally, the noise is calculated by averaging the 12 standard deviation values from each time record. The photoacoustic signal of the first measurement of each time series is taken as background level. Figure 3 shows the calculated noise and measured background signal as a function of the irradiated laser power.

In cantilever enhanced photoacoustic spectroscopy, noise originates from several sources: acceleration noise also known as vibrational noise, acoustical noise, electrical noise, background signal instability and the ultimate limiting Brownian noise [11, 29, 30]. In practice, the electrical noise level can be kept below all the other above mentioned noise types [11]. In case the vibration and acoustical disturbances from the surroundings are eliminated,

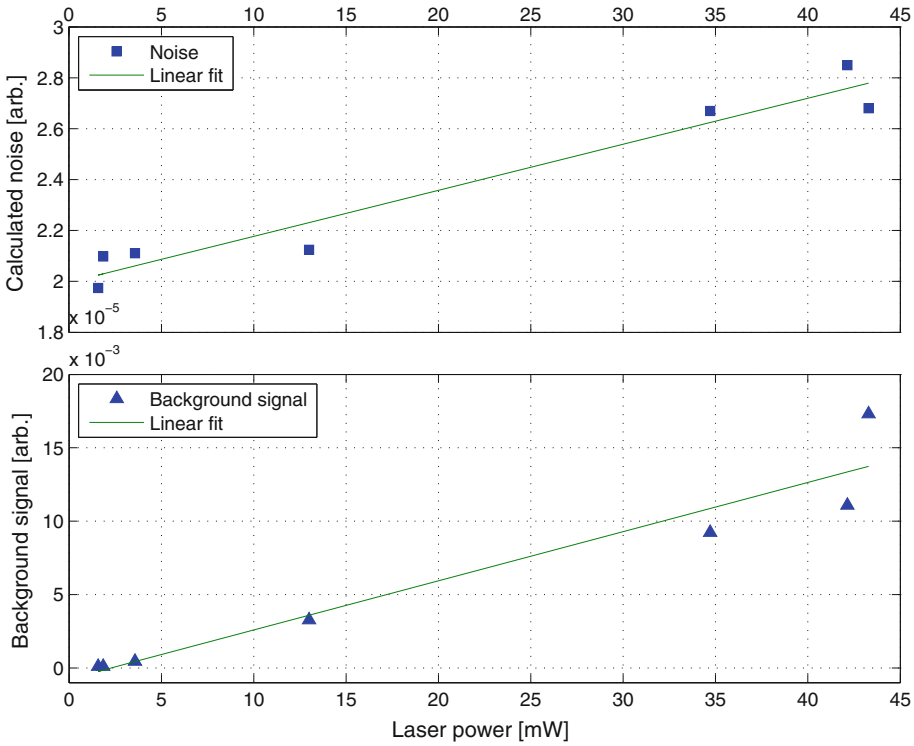

Fig. 3 Noise and background signal versus the irradiated laser power

Brownian noise and background signal instability are the main noise sources [11, 29]. This is in agreement with the here performed measurements where vibrational and acoustical noise were not observed. The background signal is generated by the photoacoustic cell walls, windows, and dust particles inside the cell. Background signal instability describes the variation of the background signal that is induced by the variation of the light source intensity and the precision of the cantilever read-out. As in case here, where the light source is a laser, the intensity variation of the source is described as the relative intensity noise (RIN) of the laser. RIN states the instability in the laser's power, to which different individual noise sources contribute [31]. The noise floor of 1.99×10^{-5} (regression line ordinate intercept), as it can be seen in Fig. 3, is due Brownian noise. The Brownian noise level was verified with a measurement where the laser was switched off. The increase in noise with increasing laser power is due to the higher background signal level.

3.2 Univariate data analysis

3.2.1 Amplitude modulation

In AM mode, the laser was tuned from 1,772 to 1,777 cm^{-1} in steps of 0.018 cm^{-1} to record the photoacoustic spectrum of formaldehyde. The measured spectrum matches the formaldehyde spectrum modeled with HITRAN [32] fairly well. The two spectra look very similar when the shape of the absorption bands is compared. The band position matches for most bands, although some bands show slight deviations due to the partially nonlinear wavelength tuning of the laser. The band intensities cannot directly be compared, and these are dependent on the instrument response curve, which is here mainly influenced by the emitted laser power. The measured formaldehyde spectrum shows two water bands, which were subtracted with a measured water spectrum. The measured and the modeled formaldehyde spectrum as well as the laser emission power function are shown in Fig. 4.

For calculating the detection limit and the normalized noise equivalent absorption coefficient (NNEA) in the univariate case, the background corrected formaldehyde band at 1,773.959 cm^{-1} is used. The noise for the AM measurement was calculated from the noise regression line (from Fig. 3) at the laser power of 47 mW (at 1,773.959 cm^{-1}). The detection limit and NNEA as well as all the parameters used for the calculation are shown in Table 1 in the column titled "AM". The detection limit (3σ, 0.951 s) is 1.6 ppbv and the NNEA (3σ) 7.32×10^{-10} W cm^{-1} $(Hz)^{-1/2}$.

3.2.2 Wavelength modulation

In WM mode, the formaldehyde spectrum was recorded from 1,772 to 1,777 cm^{-1} in steps of 0.018 cm^{-1} with a modulation amplitude of 0.15 cm^{-1}, which corresponds, to a modulation index of 1.5 for the 1,773.959 cm^{-1} band.

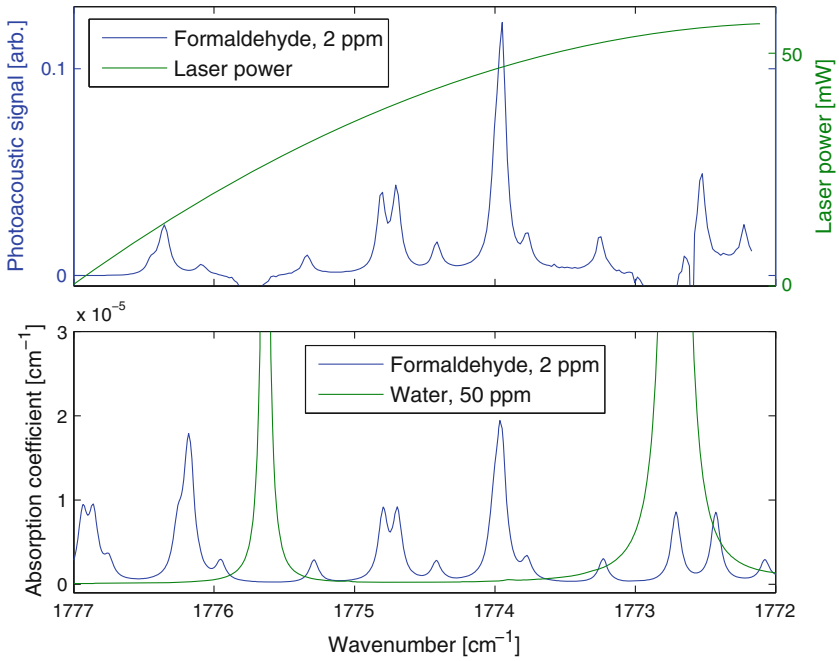

Fig. 4 *Upper graph* measured amplitude modulated formaldehyde spectrum at 2 ppmv, and the laser power emission curve. The spectrum of formaldehyde contains negative elements, which are residuals of the water subtraction. *Lower graph* absorption coefficient of 2 ppm formaldehyde and 50 ppm water at 350 mbar and 323.15 K, modeled with HITRAN [32]

Table 1 Parameters and results for the calculation of the detection limit and the NNEA in amplitude modulation (AM) and wavelength modulation (WM)

	AM	WM
Laser power, P (mW)	47.0	47.0
Formaldehyde concentration, c (ppmv)	2.00	2.00
Wavenumber, ν (cm^{-1})	1,773.959	1,773.959
Signal, S (arb.)	0.105	0.089
Noise (1σ), N (arb.)	2.85×10^{-5}	1.99×10^{-5}
Measurement time, t (s)	0.951	0.951
Signal to noise ratio, SNR (3σ)	1,225	1,486
Detection limit (3σ) (ppbv)	1.6	1.3
Absorption path length, l (cm)	9.50	9.50
Absorption coefficient (2 ppm, 350 mbar, 323.15 K), α (cm^{-1})	1.96×10^{-5}	1.96×10^{-5}
Minimum detectable absorption coefficient (3σ), α_{min} (cm^{-1})	1.60×10^{-8}	1.32×10^{-8}
Minimum detectable optical density (3σ), $\alpha_{min}\ l$	1.52×10^{-7}	1.25×10^{-7}
NNEA (3σ) [W cm^{-1} $(Hz)^{-1/2}$]	7.32×10^{-10}	6.04×10^{-10}

The measured wavelength modulated formaldehyde spectrum is shown in Fig. 5.

For the detection limit and NNEA calculation, the same band as for AM was used but no water and background subtraction was necessary. The noise for WM was taken from the ordinate intercept of the noise regression line (from Fig. 3), because of the absence of the background noise. The detection limit and NNEA as well as all the parameters used for the calculation are shown in Table 1 in the column titled "WM". The detection limit (3σ, 0.951 s) is 1.3 ppbv and the NNEA (3σ) 6.04×10^{-10} W cm^{-1} $(Hz)^{-1/2}$.

The detection limit in WM improved by a factor of 1.23 as compared to AM, although the signal height in wavelength is lower than in AM. The reason for that is the lower noise level when measuring with WM. The lower signal is due to the redistribution of the $2f_{mod}$ signal to higher harmonics and the modulation index of 1.5. For triangular modulation, the modulation index for maximal signal in the second harmonic is reported to be 2.8 by Iguchi [33] and 3.0 by Saarela et al. [34].

3.3 Multivariate analysis

Multivariate data analysis was done using science-based calibration (SBC). Derivation, formulas and application examples are reported in [35–38].

In general, multivariate analysis improves the system performance, if the analyte specific absorption band is supported by more than one data point. Multivariate data analysis is particularly suited for measurement systems where additional spectral points are acquired without increasing the measurement time, e.g. in FT-IR's or grating instruments. In laser-based systems additional measured points increase the measurement time. As so in the study here, where multivariate detection does not improve the detection limits as compared to univariate if scaled on measurement time. This comes from the fact that the measurement points on the side of the analyte band have a lower SNR than at the band maximum. Therefore, multivariate detection and data analysis is justified only if a

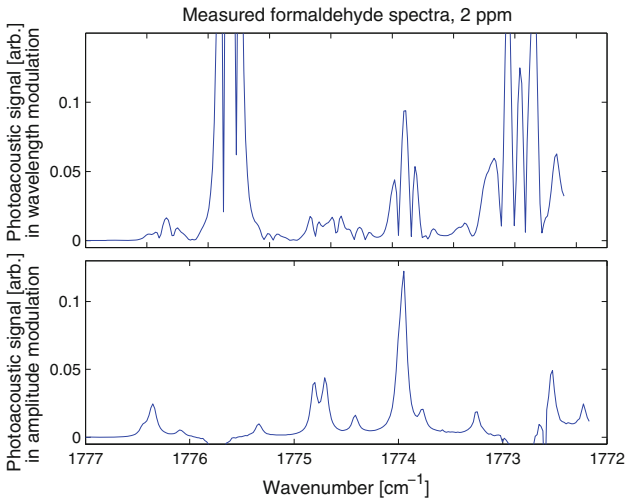

Fig. 5 *Upper graph* measured wavelength modulated formaldehyde spectrum at 2 ppmv. *Lower graph* measured amplitude modulated formaldehyde spectrum at 2 ppmv to support comparison and band allocation of the wavelength modulated spectrum

particular reason calls for it, as e.g. interferents overlapping with the analyte band. Here, multivariate data analysis can reach a detection limit (3σ) of 623 pptv (1,773.743–1,774.265 cm^{-1}, 30 spectral points each 0.951 s) for WM and 901 pptv (1,773.833–1,774.085 cm^{-1}, 15 spectral points each 0.951 s) for AM.

3.4 Future system enhancements

Several options were evaluated to improve the measurement system performance:

1. Optimization of the modulation index and the use of a different WM waveform. Iguchi [33] and Saarela et al. [34] reported that the $2f_{\mathrm{mod}}$ signal can be increased by changing the waveform to quasi-square or shaped. According to Saarela et al. [34], the photoacoustic signal improves by a factor of 1.40 for quasi-square and 1.27 for shaped compared to the triangular waveform.
2. The time-domain signal of the cantilever displacement is transferred to the frequency domain via FFT power density calculation. Using a phase-sensitive detection, will improve the performance by a factor of $\sqrt{2}$. A further factor of $\sqrt{2}$ in performance can be gained by reading the signal with a lock-in amplifier instead, as one of the components sine or cosine is eliminated. The overall performance improvement can be as high as about factor 2.
3. Adjusting the wavelength of the QCL to the formaldehyde absorption band with the highest absorption coefficient. The highest absorption coefficient in the region between 1,620 and 1,840 cm^{-1} is at 1,769.466 cm^{-1} and has a 1.10 times higher absorption coefficient as used in this study. For AM, the Q-branch of the vibrational level with an FWHM $\approx$ 0.5 cm^{-1} occurring at 1,745.826 cm^{-1} is a factor of 1.38 higher.
4. Water vapor in concentrations higher than 100 ppb disturb the formaldehyde detection in AM, because the water bands grow and, by that, affect the formaldehyde band sitting on the tail of the water band as can be seen in Fig. 4. Therefore, the signal increase due to the absorption of water needs to be subtracted. This can be realized, in a second spectral measurement point between the formaldehyde and the water bands where formaldehyde does not anymore absorb. In this way, the formaldehyde quantification can be corrected from the interference of water. Assuming the same measurement time for both spectral points, only half of the measurement time can be spent to measure the analyte; that will result in a factor of $\sqrt{2}$ worse detection limit.
5. Increase the laser's optical power. CW DFB QCLs with powers up to 300 mW are commercially available. The target is to optimize the laser's wavelength to the wavelength of the analyte's highest absorption coefficient while increase the laser output power. Owing to increasing background signal in AM, WM will benefit more from an increase in the laser power.

In prospect all the enhancements will be used, the univariate detection limit (3σ, 0.951 s) in AM can be as low as 0.36 and 0.07 ppbv for WM. If further improvement of the detection limit is required, the measurement time can be increased.

3.5 Review of previous work in the field of photoacoustic formaldehyde detection

Horstjann et al. [39] reported the detection and quantification of formaldehyde using quartz-enhanced photoacoustic spectroscopy (QEPAS) with a mid-infrared DFB interband cascade laser. The laser had an output power of 12 mW at 2,832.483 cm^{-1} and needed to be cooled down to 78 K. With a Q-factor of 16,725, a detection limit (1σ) of 0.6 ppm and NNEA (1σ) of 2.2×10^{-8} W cm^{-1} (Hz)$^{-1/2}$ were achieved for 10 s measurement time. Angelmahr et al. [40] developed a photoacoustic system based on the grazing-incidence optical parametric oscillator as light source. At 2,805.0 cm^{-1} and a Q-factor of 31 ± 2, the reported detection limit (1σ) of formaldehyde is 3 ppbv and the NNEA (1σ) 6.2×10^{-9} W cm^{-1} (Hz)$^{-1/2}$ for 3 s lock-in time constant and 3 min acquisition time. Elia et al. [41] built a photoacoustic system based on the thermoelectrically cooled DFB QCL and a resonant photoacoustic cell equipped with four electret microphones. The system reached a formaldehyde detection limit (1σ) of 150 ppbv and an

NNEA (1σ) of 2.0×10^{-8} W cm^{-1} (Hz)$^{-1/2}$ for 10 s of measurement time. The laser had an optical output power of 4 mW and the wavelength measured at was 1,778.9 cm^{-1}. Cihelka et al. [42] set-up a resonant photoacoustic system with an InAsSb/InAsSbP laser operating at a temperature of 62 K. The detection of formaldehyde was done at 2,821.76 and 2,821.79 cm^{-1}. With a measurement time of 150 s, a detection limit of 10 ppbv was reached.

One main difference of the studies listed above and the here presented study is the use of resonance enhancement. The use of resonant cells improves the performance of the photoacoustic system, but makes the system design more complicated, due to the fact that the resonance frequency needs to be precisely adjusted and kept constant over time. Using the cantilever microphone, as done here, no resonance enhancement is necessary and still the NNEA is minimum one magnitude better than reported in the studies referred above. Further, the photoacoustic system presented here fits in a 19″ rack, does not require liquid nitrogen cooling, is man-portable and can be used in industrial measurements.

4 Summary

In this study, a novel combination of cantilever enhanced photoacoustic spectroscopy with mid-infrared QCL was demonstrated. The QCL was tunable in the spectral range from 1,772 to 1,777 cm^{-1} at 18 °C. This range suits very well for the detection of formaldehyde, due to its rich rotational spectrum. The band at 1,773.959 cm^{-1} was selected for data analysis, because it is the band with the highest absorption coefficient that the laser could reach. With a laser power of 47 mW and a measurement time of 0.951 s, a univariate detection limit (3σ) of 1.6 ppbv for AM and 1.3 ppbv for WM was achieved. The calculated NNEA (3σ) for AM is 7.32 and 6.04×10^{-10} W cm^{-1} (Hz)$^{-1/2}$ for WM. Multivariate data analysis can improve the detection limits at the expense of measurement time. By means of multivariate data analysis using the SBC, the detection limit (3σ) can be improved to 623 pptv with 30 spectral points each 0.951 s for WM and 901 pptv with 15 spectral points each 0.951 s for AM.

Future improvements as using a different WM waveform, reading the phase sensitive photoacoustic signal with an lock-in amplifier, optimizing the wavenumber of the QCL to the band with the highest absorption coefficient, resolving the interference of water and increasing the laser power were evaluated. In case all improvements will be implemented and perform as estimated, the univariate detection limit (3σ, 0.951 s) is 0.36 ppbv for AM and 0.07 ppbv for WM.

The built system suites for most of the applications listed in the introduction. It reached sub-ppb detection limits, and it fits in a 19″ rack, needs only a power supply and water cooling. With minor modifications, as e.g. the sampling system, the here presented measurement system is ready for most of the listed measurement applications, including industrial and process gas measurement of formaldehyde, environmental as well as indoor and urban area formaldehyde monitoring.

Acknowledgments The authors acknowledge the financial support of the Graduate School in Chemical Engineering, Finland and III-V lab for providing the QCL source within the CUSTOM FP7 EU project.

References

1. WHO: formaldehyde, concise international chemical assessment document 40: Geneva (2002), http://www.inchem.org. Accessed 4 Mar 2013
2. I.M. Ritchie, R.G. Lehnen, Am. J. Public Health **77**, 323 (1987)
3. T. Malaka, A.M. Kodama, Arch. Environ. Health **45**, 288 (1990)
4. T. Salthammer, S. Mentese, R. Marutzky, Chem. Rev. **110**, 2536 (2010)
5. K.T. Morgan, Toxicol. Pathol. **24**, 291 (1997)
6. C. Wang, P. Sahay, Sens. Basel **9**, 8230 (2009)
7. A. Wehinger, A. Schmid, S. Mechtcheriakov, M. Ledochowski, C. Grabmer, G.A. Gastl, A. Amann, Int. J. Mass Spectrom. **265**, 49 (2007)
8. Finnish Institute of Occupational Health: formaldehyde: effects to health and exposure (2011), http://www.ttl.fi/fi/kemikaaliturvallisuus/ainekohtaista_kemikaalitietoa/formaldehydi/formaldehydin_terveysahaitat_ja_ltistuminen/sivut/default.aspx. Accessed 4 Mar 2013
9. K. Wilcken, J. Kauppinen, Appl. Spectrosc. **57**, 1087 (2003)
10. J. Kauppinen, K. Wilcken, I. Kauppinen, V. Koskinen, Microchem. J. **76**, 151 (2004)
11. T. Kuusela, J. Kauppinen, Appl. Spectrosc. Rev. **42**, 443 (2007)
12. J. Fonsen, V. Koskinen, K. Roth, J. Kauppinen, Vib. Spectrosc. **50**, 214 (2009)
13. J. Kauppinen, V. Koskinen, J. Uotila, I. Kauppinen, Proc. SPIE **5617**, 115 (2004)
14. T. Kuusela, J. Peura, B.A. Matveev, M.A. Remennyy, N.M. Stus', Vib. Spectrosc. **51**, 289 (2009)
15. A.M. Parkes, K.A. Keen, E.D. McNaghten, Proc. SPIE **6770**, 67701C (2007)
16. V. Koskinen, J. Fonsen, K. Roth, J. Kauppinen, Appl. Phys. B Lasers Opt. **86**, 451 (2007)
17. T. Laurila, H. Cattaneo, T. Pöyhönen, V. Koskinen, J. Kauppinen, R. Hernberg, Appl. Phys. B Lasers Opt. **83**, 285 (2006)
18. T. Laurila, H. Cattaneo, V. Koskinen, J. Kauppinen, R. Hernberg, Opt. Express **13**, 2453 (2005)
19. H. Cattaneo, T. Laurila, R. Hernberg, Appl. Phys. B Lasers Opt. **85**, 337 (2006)
20. C.B. Hirschmann, J. Uotila, S. Ojala, J. Tenhunen, R.L. Keiski, Appl. Spectrosc. **64**, 293 (2010)
21. C.B. Hirschmann, N.S. Koivikko, J. Raittila, J. Tenhunen, S. Ojala, K. Rahkamaa-Tolonen, R. Marbach, S. Hirschmann, R.L. Keiski, Sens. Basel **11**, 5270 (2011)
22. J. Uotila, J. Kauppinen, Appl. Spectrosc. **62**, 655 (2008)
23. J. Uotila, Eur. Phys. J Spec. Top. **153**, 401 (2008)
24. J. Uotila, Infrared Phys. Technol. **51**, 122 (2007)
25. J. Uotila, V. Koskinen, J. Kauppinen, Vib. Spectrosc. **38**, 3 (2005)

26. I. Kauppinen, A. Branders, J. Uotila, S. Sinisalo, J. Kauppinen, T. Kuusela, Tech. Mess. **79**, 17 (2012)
27. V. Koskinen, J. Fonsen, J. Kauppinen, I. Kauppinen, Vib. Spectrosc. **42**, 239 (2006)
28. R.E. Lindley, A.M. Parkes, K.A. Keen, E.D. McNaghten, A.J. Orr-Ewing, Appl. Phys. B Lasers Opt. **86**, 707 (2007)
29. V. Koskinen, J. Fonsen, K. Roth, J. Kauppinen, Vib. Spectrosc. **48**, 16 (2008)
30. J. Uotila, *Use of the Optical Cantilever Microphone in Photoacoustic Spectroscopy* (University of Turku, Turku, 2009)
31. T. Gensty, W. Elsäßer, Opt. Commun. **256**, 171 (2005)
32. L.S. Rothman, I.E. Gordon, A. Barbe, D.C. Benner, P.F. Bernath, M. Birk, V. Boudon, L.R. Brown, A. Campargue, J.-P. Champion, K. Chance, L.H. Coudert, V. Dana, V.M. Devi, S. Fally, J.-M. Flaud, R.R. Gamache, A. Goldman, D. Jacquemart, I. Kleiner, N. Lacome, W.J. Lafferty, J.-Y. Mandin, S.T. Massie, S.N. Mikhailenko, C.E. Miller, N. Moazzen-Ahmadi, O.V. Naumenko, A.V. Nikitin, J. Orphal, V.I. Perevalov, A. Perrin, A. Predoi-Cross, C.P. Rinsland, M. Rotger, M. Šimečková, M.A.H. Smith, K. Sung, S.A. Tashkun, J. Tennyson, R.A. Toth, A.C. Vandaele, J. Vander Auwera, J. Quant. Spectrosc. Radiat. Transf **110**, 533 (2009)
33. T. Iguchi, J. Opt. Soc. Am. B Opt. Phys. **3**, 419 (1986)
34. J. Saarela, J. Toivonen, A. Manninen, T. Sorvajärvi, R. Hernberg, Appl. Opt. **48**, 743 (2009)
35. R. Marbach, J. Biomed. Opt. **7**, 130 (2002)
36. R. Marbach, J. Near Infrared Spectrosc. **13**, 241 (2005)
37. R. Marbach, Pharm. Manuf. **6**, 42 (2007)
38. R. Marbach, Pharm. Manuf. **6**, 44 (2007)
39. M. Horstjann, Y.A. Bakhirkin, A.A. Kosterev, R.F. Curl, F.K. Tittel, C.M. Wong, C.J. Hill, R.Q. Yang, Appl. Phys. B Lasers Opt. **79**, 799 (2004)
40. M. Angelmahr, A. Miklós, P. Hess, Appl. Phys. B Lasers Opt. **85**, 285 (2006)
41. A. Elia, C. Di Franco, V. Spagnolo, P.M. Lugarà, G. Scamarcio, Sens. Basel **9**, 2697 (2009)
42. J. Cihelka, I. Matulková, S. Civiš, J. Mol. Spectrosc. **256**, 68 (2009)